Nucleophilic Activation of Coordinated Carbon Monoxide. 2. Reactions of the Mononuclear Complexes $M(CO)_5$ [M = Fe, Ru, or Os] with Hydroxide and with Methoxide[1,2]

Raymond J. Trautman, David C. Gross,* and Peter C. Ford*

Contribution from the Department of Chemistry, University of California, Santa Barbara, California 93106. *Received April 24, 1984*

Abstract: Quantitative studies of the reactions of the nucleophiles CH_3O^- and OH^- with the pentacarbonyl complexes $M(CO)_5$ [M = Fe, Ru, Os] are described. For methoxide the product in each case is the methoxycarbonyl adduct $M(CO)_4(CO_2CH_3)^-$. Infrared spectra in THF solution show this species to undergo specific ion pairing interaction with Na^+ at the CO_2CH_3 group. The rates of $NaOCH_3$ reaction with the metal carbonyl complexes follow the order $Os(CO)_5 > Ru(CO)_5 > Fe(CO)_5$ and are markedly solvent dependent with second-order rate constants for $Fe(CO)_5$ ranging from 1.1×10^3 M^{-1} s^{-1} in methanol to 9.7×10^4 M^{-1} s^{-1} in 90/10 (v/v) THF/CH_3OH solution (25 °C). Reaction with NaOH to give the hydroxycarbonyl adduct $M(CO)_4(CO_2H)^-$ is somewhat slower and is followed by decarboxylation to give the metal hydride complex $HM(CO)_4^-$. Detailed investigation of the decarboxylation of $Fe(CO)_4(CO_2H)^-$ has led to the conclusion that in relatively nonpolar aqueous THF solutions this step occurs via a base-independent "β-elimination", i.e., hydrogen transfer to the metal concerted with cleavage of the metal–carbon bond. The relevance of these data to the mechanism of the water gas shift reaction as catalyzed by iron carbonyls is discussed.

The homogenously catalyzed activation of carbon monoxide has been an area of intensive experimental investigation in recent years.[3] This renewed attention has been based in part upon the perceived desirability of using synthesis gas [CO/H_2 mixture] as feedstock for the production of organic chemicals and fuels. Among the reactions of interest have been CO reduction by dihydrogen,[4] reductive carbonylations of various organic substrates,[5] and the water gas shift reaction (WGSR).[5e,6] A key process in several mechanisms proposed for such catalysis cycles is the nucleophilic activation of coordinated CO, e.g., eq 1. For example,

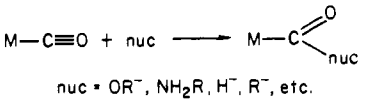

(1)

homogenous catalysis of the WGSR by metal carbonyls in alkaline solution has been proposed to proceed via a cycle such as shown in Scheme I.[7] The CO activation in this scheme is the reaction with hydroxide to give a hydroxycarbonyl complex, $M(CO_2H)^-$.

Scheme I

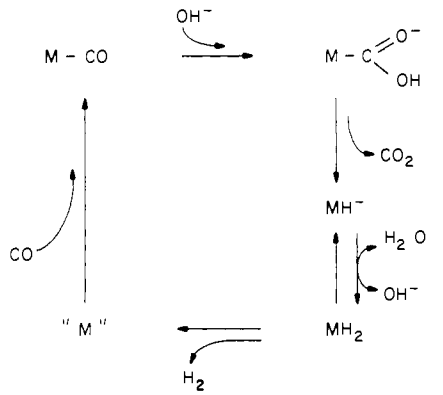

Subsequent decarboxylation would lead to formation of the metal hydride anion MH^-. Notably, catalytic activation of CO via such reactions with H_2O or base has importance not only for the WGSR adjustment of CO/H_2 ratios in synthesis gas feedstocks but also as a methodology for using carbon monoxide/water mixtures for the catalytic reduction and hydroformylation/hydroxymethylation of various organic substrates.[4a,c,8]

A major emphasis of this laboratory has been to evaluate quantitatively fundamental reactions which may have importance in homogeneous catalysis. Examples are the individual steps of Scheme I which need characterization in order to determine the validity of the overall cycle as a mechanism for WGSR catalysis. Furthermore, once the kinetics and thermodynamics of such individual steps have been characterized as functions of systematic variables, it should be possible to predict conditions under which such a cycle will operate optimally.

In the context of these goals, we have reported previously upon the kinetics and equilibria of the proton transfer reactions of several mono- and polynuclear group 8 metal carbonyl hydride complexes.[9] In the present manuscript, we describe the quantitative investigations of the reaction of hydroxide with the pentacarbonyl

(1) Part 1 was the preliminary communication: Gross, D. C.; Ford, P. C. *Inorg. Chem.* **1982**, *21*, 1702-1704.
(2) Taken in part from the Ph.D. dissertation of D. C. Gross, UCSB, 1983.
(3) See, for example, articles in the following: (a) Ford, P. C., Ed. "Catalytic Activation of Carbon Monoxide"; American Chemical Society: Washington, D.C., 1981; ACS Symp. *Ser.* Vol. 152. (b) Keim, W., Ed. "Catalysis in C_1 Chemistry"; A. Reidel Publishers: Dorchecht, Holand, 1983. (c) Parshall, G. W. "Homogeneous Catalysis"; Wiley-Interscience: New York, 1981. (d) Masters, C. "Homogeneous Transiton Metal Catalysis"; Chapman and Hall, Publishers: London, 1981.
(4) (a) Doxsee, K. M.; Grubbs, R. H. *J. Am. Chem. Soc.* **1981**, *103*, 7696-7698. (b) Stewart, R. P.; Okomato, N.; Graham, W. A. G. *J. Organomet. Chem.* **1972**, *42*, C32. (c) Casey, C. P.; Neumann, S. M. *J. Am. Chem. Soc.* **1976**, *98*, 5395-5396. (d) Tam, W.; Wong, W.-K.; Gladysz, J. A. *J. Am. Chem. Soc.* **1979**, *101*, 1589. (e) Chen, M. J.; Feder, H. M.; Rathke, J. W. *J. Am. Chem. Soc.* **1982**, *104*, 7346-4349.
(5) (a) von Kutepow, N.; Kindler, H. *Angew. Chem.* **1960**, *72*, 802-805. (b) Laine, R. M. *J. Am. Chem. Soc.* **1978**, *100*, 6451-6454. (c) Alper, H.; Hashem, K. E. *J. am. Chem. Soc.* **1981**, *103*, 6514-6515. (d) Kang, H.; Mauldin, C. H.; Cole, T.; Slegeir, W.; Cann, K., Pettit, R. *J. Am. Chem. Soc.* **1977**, *99*, 8323. (e) Pruett, R. *Adv. Organomet. Chem.* **1979**, *17*, 1-60.
(6) (a) Laine, R. M.; Rinker, R. G.; Ford, P. C. *J. Am. Chem. Soc.* **1977**, *99*, 252. (b) Cheng, C. H.; Hendricksen, D.; Eisenberg, R. *J. Am. Chem. Soc.* **1977**, *99*, 2791. (c) King, R. B.; Frazier, C. C.; Hanes, R. M.; King, A. D. *J. Am. Chem. Soc.* **1978**, *100*, 2925. (d) Darensbourg, D. J.; Darensbourg, M. Y.; Burch, R. R.; Froelich, J. A.; Incorvia, M. J. *Adv. Chem. Ser.* **1979**, *173*, 106. (e) Ford, P. C.; Rinker, R. G.; Laine, R. M.; Ungermann, C.; Landis, V.; Moya, S. A. *J. Am. Chem. Soc.* **1978**, *100*, 4595.
(7) (a) Ford, P. C. *Acc. Chem. Res.* **1981**, *14*, 31 and references therein. (b) Halpern, J. *Comments Inorg. Chem.* **1981**, *1*, 3 and references therein.
(8) (a) Cheng, C. H.; Kuritzkes, L.; Eisenberg, R. *J. Organomet. Chem.* **1980**, *190*, C21. (b) Cole, T.; Ramage, R.; Cann, K.; Pettit, R. *J. Organomet. Chem.* **1980**, *190*, C21. (c) Cole, T.; Ramage, R.; Cann, K.; Pettit, R. *J. Am. Chem. Soc.* **1980**, *102*, 6182-6184. (d) Fish, R. H.; Thormodsen, A. D.; Cremer, G. A. *J. Am. Chem. Soc.* **1982**, *104*, 5234-5237.
(9) Walker, H. W.; Pearson, R. G.; Ford, P. C. *J. Am. Chem. Soc.* **1983**, *105*, 1179-1186.

0002-7863/85/1507-2355$01.50/0

complexes $M(CO)_5$ [eq 2, M = Fe or Ru] and of the subsequent decarboxylation (eq 3).

$$M(CO)_5 + OH^- \rightleftharpoons M(CO)_4(CO_2H)^- \quad (2)$$

$$M(CO)_4(CO_2H)^- \rightarrow HM(CO)_4^- + CO_2 \quad (3)$$

In addition the reactions of $M(CO)_5$ [M = Fe, Ru, and Os] with methoxide to give the respective methoxycarbonyl adducts (eq 4) were also investigated as a model for eq 2. Another study[10] has described similar investigations for $Fe(CO)_5$ in aqueous methanol; however, the present work represents a much broader investigation, including other metal complexes and solvent conditions. A separate article[11] of this series describes analogous studies for the triangular clusters $M_3(CO)_{12}$ [M = Fe, Ru, and Os].

$$M(CO)_5 + CH_3O^- \rightleftharpoons M(CO)_4(CO_2CH_3)^- \quad (4)$$

Experimental Section

Materials. Carbon monoxide (C.P. grade), argon, and nitrogen, supplied by Linde, were purified by passing them through a heated column of BASF Deox catalyst and then through a column of molecular sieve and Drierite. All manipulations were carried out under a CO atmosphere with standard Schlenk techniques unless stated otherwise. Tetrahydrofuran (THF) was distilled from sodium–benzophenone; hexane and methanol were distilled from CaH_2. Solutions were purged with the desired gas (~1-min purge per 1 mL of solvent) or first degassed with 3 freeze–pump–thaw (f-p-t) cycles and then stirred under the appropriate gas. Deuterated solvents were purchased from Aldrich or Stohler Isotopes and handled in the same fashion as the perprotio analogues. Water was doubly distilled and degassed with four f-p-t cycles. All mixed solvents for kinetics studies were prepared in volume-to-volume ratios.

Bis(triphenylphosphoranylidene)ammonium chloride, (PPN)Cl, was obtained from Aldrich and dried in vacuo at 100 °C for a minimum of 3 h prior to use. Iron pentacarbonyl (Alfa) was distilled in vacuo and stored cold under CO in the dark. Ruthenium pentacarbonyl was prepared by the high-pressure reaction of $Ru_3(CO)_{12}$ with CO.[12] In a typical preparation, a 70-mg sample of $Ru_3(CO)_{12}$ in 30 mL of THF was introduced into a Paar high-pressure autoclave. This apparatus was pressurized to ~1300 psi of CO and stirred at 160 °C overnight. After the apparatus was cooled to room temperature, the reactor was connected to a vacuum line and all volatiles distilled into a dry ice/acetone cooled trap. The THF solution of $Ru(CO)_5$ thus obtained was stored under CO in the dark at −78 °C to prevent cluster formation. Osmium pentacarbonyl was prepared from the high-pressure reaction of OsO_4 (Aldrich) and CO in a manner analogous to that for $Ru(CO)_5$.[12]

Methanolic $NaOCH_3$ was prepared by adding freshly cleaned sodium to distilled methanol. After the reaction was complete, the solution was degassed with f-p-t cycles and stored under N_2 or Ar. Base concentration was determined by aqueous titration with HCl solutions prepared from J. T. Baker "Dilut-it" standards. The nonaqueous titrant, tetra-*n*-butylammonium hydroxide, $(Bu_4N)OH$, was obtained from Aldrich as a 1 M solution in CH_3OH or as a 40% by weight solution in water. In order to prepare the methoxide salt either the methanolic or aqueous solution (~10 mL) was transferred to a Schlenk flask and all volatiles removed in vacuo at 40 °C for several hours. The resulting clear oil was taken up in anhydrous degassed methanol (~10 mL) and stored under argon.

Synthesis of [PPN][M(CO)$_4$(CO$_2$CH$_3$)] (M = Fe, Ru, or Os). The methoxycarbonyl complexes were prepared by reaction of $NaOCH_3$ with the metal pentacarbonyl under stringently dry conditions. The sodium salts were not isolated from solution. The PPN^+ salts were isolated as described here for the ruthenium complex.

[PPN][Ru(CO)$_4$(CO$_2$CH$_3$)]. $NaOCH_3$ (1 M in CH_3OH, 0.5 mL; 0.5 mmol) was added to a THF solution of $Ru(CO)_5$ (~0.35 mmol). Dry [PPN]Cl (287 mg, 0.5 mmol) dissolved in the minimum volume of anhydrous methanol (~2 mL) was immediately added to the solution with stirring against a stream of CO. All volatiles were subsequently removed by vacuum distillation. The remaining material was chilled to −78 °C and washed at this temperature with several 2-mL portions of anhydrous methanol. The light yellow solid was then taken up in THF (~3 mL), passed through a fine frit, and crystallized by the slow addition of hexane. The product was collected by filtration, dried under vacuum, and stored under CO. Yield, based on initial moles of $Ru_3(CO)_{12}$, was 65%. Anal. Calcd for $C_{42}H_{33}NO_6P_2Ru$: C, 62.22; H, 4.07. Found: C, 61.42; H, 4.14. ^1H NMR: [$(CD_3)_2SO$, δ, relative integration] 3.10 (1), ~7.0 multiplet (10).

[PPN][Fe(CO)$_4$(CO$_2$CH$_3$)]. This compound is much more susceptible to moisture than are the Ru and Os analogues. The salt was recrystallized in 70% yield from THF/hexane and displayed properties identical with those reported previously.[13]

[PPN][Os(CO)$_4$(CO$_2$CH$_3$)]. This was prepared in a manner analogous to that described for the iron complex. Anal. Calcd for $C_{42}H_{33}NO_6P_2Os$: C, 56.06; H, 3.67. Found: C, 55.19; H, 3.86.

[PPN][$HRu(CO)_4$][14] and [PPN][$HFe(CO)_4$][15] were prepared following literature procedures. $Ru(CO)_4(P(OCH_3)_3)$ was prepared by the thermal substitution of $Ru(CO)_5$.[16] A 30-mg portion of $Ru_3(CO)_{12}$ was dissolved in 150 mL of hexane. This solution was photolyzed at ~4 °C with a Hanovia lamp under a stream of CO until the solution was colorless. The resulting hexane solution of $Ru(CO)_5$ was vacuum distilled into a dry ice/acetone cooled trap. After the mixture was warmed to room temperature, a tenfold excess of $P(OCH_3)_3$ was added and the solution stirred overnight. The resulting pale yellow solution was evaporated under vacuum to dryness. The solid was taken up in ~10 mL of hexane, and the solution was filtered and then cooled to −80 °C, yielding white crystalline $Ru(CO)_4(P(OCH_3)_3)$. Infrared and ^1H NMR spectra agreed with published values.[16]

Instrumentation. Electronic and infrared spectra were obtained with Cary 118C and Perkin-Elmer 683 spectrophotometers, respectively. NMR spectra were obtained on a Varian XL-100, CFT-20, or Nicolet NT300 spectrometer. Deuterated solvents were used for both lock and internal calibration.[17] Stopped-flow kinetics studies were carried out with a Durrum-Gibson D110 stopped-flow UV-vis spectrophotometer equipped with a constant temperature water bath and with a Biomation 805 transient digitizer interfaced to a Hewlett-Packard 86 microcomputer for collection and analysis of data. Solutions for kinetics studies were prepared from stock metal carbonyl and base solutions and were transferred via syringes to the stopped-flow spectrophotometer syringes under N_2 or CO. some rate studies were carried out with the Perkin-Elmer 683 infrared spectrophotometer equipped with a stopped-flow cell configuration for rapid mixing of reaction solutions (dead time ~2 s) and interfaced to the transient digitizer and computer noted above.

Rate data were analyzed from ln $(A_t - A_\infty)$ vs. t plots (linear least-squares fit) or from the kinetic over-relaxation method (KORE) of Swain et al.[18] The latter method was essential for data sets with a poor signal-to-noise ratio.

Table I. Infrared Data in the CO Stretching Region for the Na^+ and PPN^+ Salts of the Methoxycarbonyl Complexes $M(CO)_4(CO_2CH_3)^-$ (M = Fe, Ru, or Os)[a]

compound	ν_{CO} terminal CO	ν_{CO} CO_2CH_3 group
$Na[Fe(CO)_4(CO_2CH_3)]$	2023 w, 1929 m, 1913 s, 1901 sh	1585 w
$(PPN)[Fe(CO)_4CO_2CH_3]$	2018 w, 1917 sh, 1903 s	1621 w
$Na[Ru(CO)_4CO_2CH_3]$	2033 w, 1944 m, 1921 s, 1906 sh	1592 w
$(PPN)[Ru(CO)_4CO_2CH_3]$	2024 w, 1929 m, 1909 s	1627 w
$Na[Os(CO)_4CO_2CH_3]$	2032 w, 1938 m, 1910 s br	1594 w
$(PPN)[Os(CO)_4(CO_2CH_3)]$	2025 w, 1926 m, 1904 s	1630 w

[a] Spectra recorded in THF solution.

Results and Discussion

I. Infrared Spectra of Methoxycarbonyl Adducts. Addition of methoxide (typically as $NaOCH_3$ in dry methanol) to $M(CO)_5$ (M = Fe, Ru, or Os) in THF or methanol gave the respective methoxycarbonyl derivatives $M(CO)_4(CO_2CH_3)^-$. These anions

(10) Pearson, R. G.; Mauermann, H. *J. Am. Chem. Soc.* **1982**, *104*, 500.
(11) Gross, D. C.; Ford, P. C. *J. Am. Chem. Soc.* **1985**, *107*, 585.
(12) Calderazzo, F.; L'Eplattenier, F. *Inorg. Chem.* **1967**, *6*, 1220.
(13) McClean, J. L. Ph.D. Dissertation, City University of New York, 1975.
(14) Walker, H. W.; Ford, P. C. *J. Organomet. Chem.* **1981**, *214*, C43.
(15) Darensbourg, M. Y.; Darensbourg, D. J.; Barros, H. L. C. *Inorg. Chem.* **1978**, *17*, 297.
(16) Cobbeldick, R. E.; Einstein, F.; Pomeroy, R. K.; Spetch, E. P. *J. Organomet. Chem.* **1980**, *195*, 77.
(17) Residue protons in the solvent were used as an internal calibrant, peak positions are referenced to Me_4Si by adding the reported chemical shift for the solvent to the observed shift. ["Sadtler Handbook of Proton NMR spectra"; Simons, W. W.; Ed.; Sadtler Research Laboratories, Inc., Philadelphia, PA, 1978.]
(18) Swain, C. G.; Swain, M. S.; Berg, L. F. *J. Chem. Inf. Comput. Sci.* **1980**, *20*, 47.

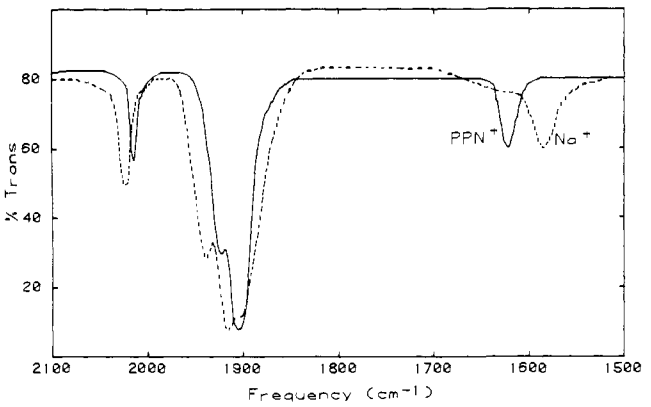

Figure 1. Infrared spectra (CO) of $[PPN][Ru(CO)_4(CO_2CH_3)]$ (solid line) and of $[Na][Ru(CO)_4(CO_2CH_3)]$ (dashed line) in THF solution.

were thermally stable but extremely moisture sensitive and were isolable as PPN^+ salts. The preparation of $Na[Fe(CO)_4(CO_2CH_3)]$ has been described previously.[13]

The IR spectra in the carbonyl region for these complexes in THF are summarized in Table I. For each complex, the three-band pattern of ν_{CO} bands is consistent with a "C_{3v}" symmetry and indicates the methoxycarbonyl group to occupy an axial site. These bands appear at higher frequencies for the Na^+ salt than for the PPN^+ salt (Figure 1). In contrast the ν_{CO} band of the methoxycarbonyl group appears at a lower frequency for the Na^+ salt than for the PPN^+ salt. These differences suggest specific interactions between the Na^+ and the CO_2CH_3 group. A and B represent resonance extremes for this group. Stabilization of the

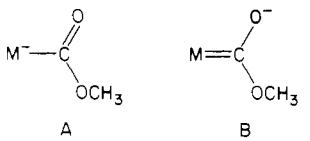

A B

latter by interaction with Na^+ at the methoxycarbonyl oxygen would raise the ν_{CO} values of terminal carbonyl groups owing to the decreased negative charge on the metal and similarly decrease $\nu_{C=O}$ for the CO_2CH_3 group. The potential importance of such counterion interaction with anionic organometallic complexes has been illustrated by Collman et al.,[19] who demonstrated that the cation had a major influence on alkyl migratory insertion reactions of $M^+[RFe(CO)_4^-]$ species. It is noteworthy that for the $M(CO)_4(CO_2CH_3)^-$ salts the terminal ν_{CO} bands occur at substantially higher frequencies than for the analogous $HM(CO)_4^-$ salts. This observation is consistent with substantial delocalization of the negative charge onto the methoxycarbonyl group, i.e., the contribution of the canonical structure B in each case. The conclusion that the $M(CO)_4(CO_2CH_3)^-$ ions have the methoxycarbonyl group in the axial position is also consistent with the proposal[20] that nucleophilic attack is favored at the CO displaying the larger force constant. Normal coordinate analyses of the IR spectra of both $Fe(CO)_5$ and $Ru(CO)_5$ have demonstrated the force constant of the axial CO group (~17.0 mdyn/Å) to be substantially larger than that of the equatorial CO group (~16.6 mdyn/Å).[21]

II. Kinetics of Reactions with Methoxide. $Ru(CO)_5$. Electronic spectral changes for the reaction of $NaOCH_3$ with $Ru(CO)_5$ are shown in Figure 2. In 10/90 THF/CH_3OH solution, successive addition of $NaOCH_3$ to $Ru(CO)_5$ resulted in a gradual change of the absorption spectrum to that of $Ru(CO)_4(CO_2CH_3)^-$, with an isosbestic point observed at 268 nm. In situ infrared spectral analysis confirmed that these electronic spectral changes represented adduct formation as shown in eq 5. An equilibrium con-

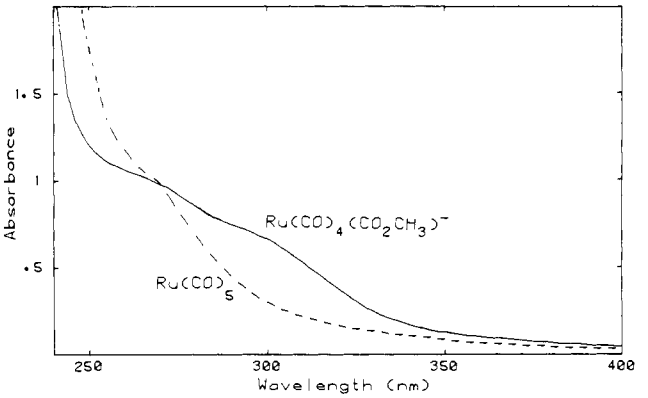

Figure 2. UV spectrum of $Ru(CO)_5$ (dashed line) and $Ru(CO)_4(CO_2CH_3)$ (solid line) in methanol.

Table II. Rate Constants for the Reaction of $Ru(CO)_5$ with $NaOCH_3$ in Various THF/CH_3OH Solvent Mixtures under CO Atmosphere

solvent[a]	T (°C)	$k_1 \times 10^{-3}$ (M^{-1} s^{-1})	k_{-1} (s^{-1})	$K_1 \times 10^{-2}$ (M^{-1})[b]
50/50	9.0	15.0 ± 0.6	18 ± 3	8 ± 2
50/50	20.6	24.1 ± 0.4	34 ± 3	7 ± 2
50/50	31.9	42.0 ± 0.5	44 ± 4	9 ± 1
	$\Delta H^\ddagger$ (kJ/mol)	30 ± 3	26 ± 6	
	$\Delta S^\ddagger$ (J/mol K)	−60 ± 8	−130 ± 20	
10/90	6.8	3.1 ± 0.1	30 ± 2	1.0 ± 0.1
10/90	19.6	5.0 ± 0.1	70 ± 7	0.7 ± 0.1 (1.1 ± 0.1)[c]
10/90	30.6	9.6 ± 0.5	105 ± 11	1.0 ± 0.1
	$\Delta H^\ddagger$ (kJ/mol)	32 ± 5	35 ± 6	
	$\Delta S^\ddagger$ (J/mol K)	−66 ± 17	−90 ± 20	

[a] THF/CH_3OH (v/v). [b] Calculated from $K_1 = k_1/k_{-1}$. [c] Measured by a static IR spectral experiment at ~23 °C.

stant $K_1 = (1.13 \pm 0.09) \times 10^2$ M^{-1} (25 °C) was determined from these static spectral measurements.

$$Ru(CO)_5 + CH_3O^- \underset{k_{-1}}{\overset{k_1}{\rightleftharpoons}} Ru(CO)_4(CO_2CH_3)^- \quad (5)$$

Reaction kinetics for eq 5 were investigated by monitoring the temporal absorbance changes (A_t) at 310 nm on the stopped-flow spectrophotometer. The concentration of $Ru(CO)_5$ was 0.03 to 0.1 mM, obtained by appropriate dilution of the stock THF solution, while that of $NaOCH_0$ was varied from ~0.1 to 50 mM, always in a large stoichiometric excess. At these base concentrations, plots of ln ($A_t - A_\infty$) vs. t were linear, thus the reactions were first order in $[Ru(CO)_5]$. Plots of k_{obsd} vs. $[NaOCH_3]$ were

$$-d[Ru(CO)_5]/dt = k_{obsd}[Ru(CO)_5] \quad (6)$$

linear (slope = k_1) with nonzero intercepts (k_{-1}) (Figure 3), consistent with the reversible adduct formation (eq 5) for which the rate law would be

$$-d[M(CO)_5]/dt = (k_1[NaOCH_3] + k_{-1})[M(CO)_5] \quad (7)$$

where

$$k_{obsd} = k_1[NaOCH_3] + k_{-1} \quad (8)$$

Values of k_1 and k_{-1} obtained in 50/50 and 10/90 THF/CH_3OH mixtures are summarized in Table II. The ratio (k_1/k_{-1}) is equal to the equilibrium constant K_1. Notably the K_1 values obtained by the kinetics method in a 10/90 THF/CH_3OH mixture are close to that measured by the static spectral method under similar conditions. Eyring plots of the temperature-dependent rate constants gave the activation parameters ($\Delta H^\ddagger$ and $\Delta S^\ddagger$) also summarized in Table II.

The reactivity of $Ru(CO)_5$ can be contrasted to that of $Ru(CO)_4(P(OCH_3)_3)$. No changes in either the UV/VIS or ν_{CO} infrared spectra were observed even 30 min after addition of $NaOCH_3$ (0.12 mmol in 20 μL of methanol) to $Ru(CO)_4(P(OCH_3)_3)$ (0.025 mmol) in 25 mL of THF. Addition of water (50

(19) Collman, J. P.; Cawse, J. N.; Brauman, J. I. *J. Am. Chem. Soc.* **1972**, *94*, 5905.
(20) Darensbourg, D. J.; Darensbourg, M. Y. *Inorg. Chem.* **1970**, *9*, 1691.
(21) (a) Bor, G. *Inorg. Chem. Acta* **1969**, *3*, 191. (b) Huggins, D.; Flitcroft, N.; Kaesz, H. D. *Inorg. Chem.* **1965**, *4*, 166.

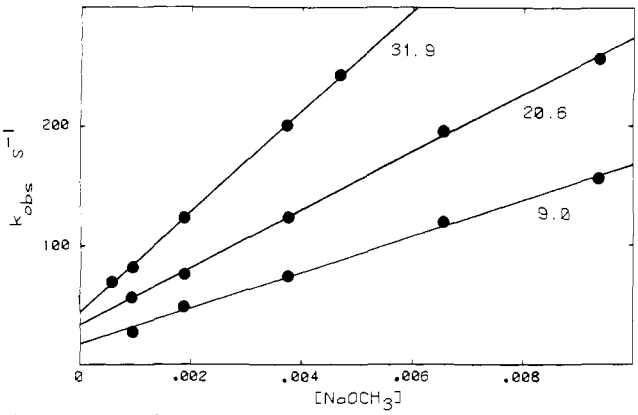

Figure 3. Plots of the first-order rate constants k_{obsd} vs. [methoxide] for the reaction of $Ru(CO)_5$ with $NaOCH_3$ as a function of temperature.

Table III. Rate Constants[a] for the Reaction of $Fe(CO)_5$ with $NaOCH_3$ in Various THF/CH_3OH Solvent Mixtures under CO Atmosphere

solvent[a]	T (°C)	$k_1 \times 10^{-3}$ (M^{-1} s^{-1})	k_{-1} (s^{-1})	$K_1 \times 10^{-2}$ (M^{-1})[b]
90/10	25.9	97.2 ± 8.8	3 ± 9	~300
90/10	14.3	64.6 ± 3.5	-15 ± 9	[c]
90/10	3.0	32.2 ± 3.8	-1 ± 8	[c]
70/30	25.0	17.6 ± 0.3	23 ± 1	7.6
50/50	25.0	7.8 ± 0.3	42 ± 2	1.9
30/70	25.0	3.5 ± 0.1	66 ± 3	0.5
10/90	25.0	1.8 ± 0.1	135 ± 8	0.13 (0.15)[d]
0/100	25.0	1.1 ± 0.1	165 ± 15	0.067 (0.055)[d]
50/48/2[e]	25.6	8.0 ± 0.2	37 ± 3	2.1

[a] THF/CH_3OH (v/v). [b] $K_1 = k_1/k_{-1}$ except where noted. [c] Experimental error in k_{-1} too large to allow estimate of K_1. [d] Determined from the IR experiment, T uncertain (see text). [e] $THF/CH_3OH/H_2O$ (v/v/v).

mmol) to the above solution resulted in the gradual decrease in intensity of the ν_{CO} bands associated with $Ru(CO)_4(P(OCH_3)_3)$. Over a period of several hours the solution developed a deep red color, possibly indicating the presence of metal hydride cluster species.

$Os(CO)_5$. Addition of sodium methoxide to THF/CH_3OH solutions of $Os(CO)_5$ resulted in electronic and ν_{CO} spectral changes similar to those shown above for reaction of $Ru(CO)_5$. Kinetic data, obtained as described above, gave the following rate constants in 5/95 THF/CH_3OH: $k_1 = (13.6 \pm 0.2) \times 10^3$ M^{-1} s^{-1}, $k_{-1} = (2.8 \pm 2.0)$ s^{-1}, and $K_1 = (4.8 \pm 3.6) \times 10^3$ M^{-1} at 25 °C.

$Fe(CO)_5$. The large differences between the k_1 values measured previously for $Fe(CO)_5$ in aqueous methanol[10] and those found here for $Ru(CO)_5$ and $Os(CO)_5$ under somewhat similar conditions prompted this reinvestigation of the $Fe(CO)_5$ system. Addition of $NaOCH_3$ in 90/10 THF/CH_3OH solution to $Fe(CO)_5$ in the same solvent results in electronic and ν_{CO} absorption changes similar to those found for the reaction with $Ru(CO)_5$. However, in solvent mixtures containing a much larger methanol concentration (approximating neat methanol), the absorbance changes were much smaller and suggested a small equilibrium constant in this solvent for the following reaction.

$$Fe(CO)_5 + CH_3O^- \rightleftharpoons Fe(CO)_4(CO_2CH_3)^- \quad (9)$$

Kinetic studies were carried out for dilute $Fe(CO)_5$ (with excess $NaOCH_3$ (0.6 ~3 × 10^{-3} M)) for a range of mixed solvents from 100% CH_3OH to 90/10 THF/CH_3OH. For all these conditions, the reaction was found to be first order in $[Fe(CO)_5]$ and plots of k_{obsd} vs. $[NaOCH_3]$ (Figure 4) were linear in analogy to eq 7. From these, k_1 and k_{-1} were determined (Table III), but in some cases the intercepts (k_{-1}) were small or negative leading to large relative experimental uncertainties in the k_{-1} values and thus in the K_1 values (determined from the k_1/k_{-1} ratio). As was seen for $Ru(CO)_5$, the rate and equilibrium constants proved markedly

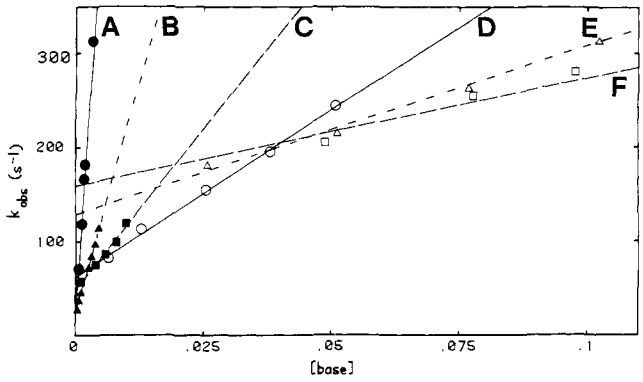

Figure 4. Plots of the first-order rate constants k_{obsd} vs. [methoxide] for the reaction of $Fe(CO)_5$ with $NaOCH_3$ as a function of solvent composition at 25 °C. Solvent system (THF/CH_3OH) (v/v): A (●) 90/10; B (▲) 70/30; C (■) 50/50; D (○) 30/70; E (△) 10/90; F (□) 0/100 (F includes higher concentration data not shown).

dependent on solvent composition. An Eyring plot gave $\Delta H^{\ddagger} = 33 \pm 4$ kJ/mol and $\Delta S^{\ddagger} = -40 \pm 15$ J/(mol K) for k_1 in 90/10 THF/CH_3OH.

The reaction of $(Bu_4N)OCH_3$ with $Fe(CO)_5$ in 90/10 THF/CH_3OH gave a k_1 value of $(2.48 \pm 0.14) \times 10^5$ M^{-1} s^{-1}, more than twice that found for $NaOCH_3$ (Table III). However, in neat methanol the reaction of $(Bu_4N)OCH_3$ with $Fe(CO)_5$ gave a k_1 value of $(1.5 \pm 0.2) \times 10^3$ M^{-1} s^{-1} that is much closer to that observed with $NaOCH_3$ [$(1.10 \pm 0.14 \times 10^3$ M^{-1} s^{-1}]. These results suggest that $NaOCH_3$ is much more extensively ion paired in 90/10 THF/CH_3OH than in neat methanol.

The K_1 measured here in neat methanol from the kinetics data was of some concern because is was more than an order of magnitude smaller than the value previously reported under similar conditions[13] and assumed by a subsequent study.[10] In order to address this concern, the equilibrium constants for eq 9 were redetermined by static infrared spectral measurements. The ratio $[Fe(CO)_4(CO_2CH_3)^-]/[Fe(CO)_5]$ was calculated over a range of $NaOCH_3$ concentrations (0.01 to 0.40 M) by measuring the $[Fe(CO)_5]$ resulting from mixing $Fe(CO)_5$ and $NaOCH_3$ solutions and assuming the difference $[Fe(CO)_5]_{initial} - [Fe(CO)_5]_{eq}$ to be $[Fe(CO)_4(CO_2CH_3^-]$. From these data the values of $K_1 = 5.5 \pm 1.2$ M^{-1} in neat methanol and 15.3 ± 1.3 M^{-1} in 10/90 THF/CH_3OH were determined. Given that there was some uncertainty in the solution temperature in the IR experiment, these results are in excellent agreement with those (6.7 and 13 M^{-1}, respectively) from the kinetics analysis.

Comparison of Rates and Equilibria. Among the three pentacarbonyl complexes investigated, the reactivity with $NaOCH_3$ follows the order Os > Ru > Fe. For a comparable set of conditions, the differences between k_1 values for the three metal compounds were relatively small (about one order of magnitude). The k_{-1} values follow the opposite order (Fe > Ru > Os), thus accentuating the range of K_1 values to more than two orders of magnitude. Given that the order of K_1 values follow that of k_1, the same factors influencing the stabilities of the methoxycarbonyl adducts are apparently dominant in determining the relative energies of the reaction transition state. Electronic factors to be considered would be the respective abilities of the various $M(CO)_4$ fragments to accommodate negative charge and the metal–ligand bonding changes in going from a strongly π-accepting CO to a stronger σ-donor but weaker π-acceptor $[CO_2CH_3^-]$ ligand. The very low reactivity of $Ru(CO)_4(P(OCH_3)_3)$ confirms the importance of such electronic effects. The reactivities of nucleophiles such as benzylmagnesium chloride with carbonyl complexes of the chromium triad show a similar pattern, i.e., W > Mo > Cr. These observations have been rationalized in terms of lesser steric constraints as well as the somewhat higher CO force constants for the heavier metal centers.[22]

(22) Darensbourg, M. Y.; Condor, H. L.; Darensbourg, D. J.; Hasday, C. *J. Am. Chem. Soc.* **1973**, *95*, 5919.

Table IV. Rate Constants for the Reaction of $(Bu_4N)OH$ with $M(CO)_5$ (M = Fe, Ru, or Os) in 90/10 THF/H_2O (v/v)[a]

compd	$k_2 \times 10^{-4}$ (M^{-1} s^{-1})	k_4 (s^{-1})[b]
$Fe(CO)_5$	1.3 ± 0.1	0.09 ± 0.02
$Fe(CO)_5$		0.07 ± 0.01[c]
$Ru(CO)_5$	1.42 ± 0.05	0.040 ± 0.006
$Os(CO)_5$	2.97 ± 0.12	not measured

[a] At 25.0 °C under 1 atm of CO. [b] First-order rate constant for the formation of $HM(CO)_4^-$ as determined in the IR experiment (see text). [c] Under 1 atm of N_2.

The solvent effects on the rate and equilibrium constants of adduct formation for both $Fe(CO)_5$ and $Ru(CO)_5$ are undoubtedly the result of a combination of parameters. As the solvent system is changed by increasing the percentage of THF, ion pairing of the reactant methoxide should be more evident with the expected effect of decreasing the intrinsic reactivity of this nucleophile. However, the methoxide ion is much more strongly solvated by the protic dipolar methanol than by THF. Thus, the dramaticaly larger values of k_1 and K_1 at the higher concentrations of THF (Table III) suggest that the destabilization of methoxide by the decreased solvating ability of the mixed solvent system more than compensates for similar effects at the reaction transition state and for any deactivation by ion pairing to Na^+.

III. Reactions with Hydroxide. Reactions in Aqueous THF and in Aqueous CH_3OH. Addition of aqueous $(Bu_4N)OH$ to THF solutions of $M(CO)_5$ [M = Fe, Ru, or Os] gave initial electronic spectral changes similar to those seen in Figure 2. However, examination of the IR spectra showed that with excess base, the sole eventual product displaying ν_{CO} bands was the respective hydride anion $HM(CO)_4^-$.[23] When the stopped-flow spectrophotometer was employed to monitor the UV spectral changes upon mixing aqueous THF solutions of $(Bu_4N)OH$ and $M(CO)_5$, three sequential absorbance changes were seen. The rates of the first two proved to be [base] dependent. The third process (believed to be metal hydride formation) appeared [base] independent; however, the spectral changes were too small to study quantitatively.

In analogy to the reaction of $M(CO)_5$ with methoxide, the first spectral change is attributed to formation of a hydroxycarbonyl adduct, eq 10. The reaction was first order in $[M(CO)_5]$, and

$$M(CO)_5 + OH^- \underset{k_{-2}}{\overset{k_2}{\rightleftharpoons}} M(CO)_4(CO_2H)^- \qquad (10)$$

plots of k_{obsd} vs. $[(Bu_4N)OH]$ were linear with nonzero intercepts, i.e., consistent with the rate law

$$-d[M(CO)_5]/dt = (k_2[OH^-] + k_{-2})[M(CO)_5] \qquad (11)$$

Values of k_2 so determined (Table IV) follow the order Os > Ru > Fe, seen also for the adduct formation with methoxide. Comparison of the $Fe(CO)_5$ reactions with $(Bu_4N)OH$ in 90/10 THF/H_2O and with $(Bu_4N)OCH_3$ in 90/10 THF/CH_3OH shows the latter system to be the more reactive (i.e., $k_1 > k_2$). Although the solvent systems are not equivalent, the greater nucleophilicity of methoxide is not unexpected.[24] The k_{-2} values were small with large relative experimental uncertainties (0 ± 5 s^{-1} so the equilibrium constants could not be determined from the kinetic data. However, it is reasonable to conclude that in each case K_2 is large (>10^3 M^{-1}), given the very large values of K_1 (>10^4 M^{-1}) obtained for $Fe(CO)_5$ under similar conditions.

The second process, which gives significant spectral changes only for reactions of $Fe(CO)_5$, was concluded to be a reaction of the hydroxycarbonyl adduct with a second hydroxide ion. The metal-containing product of this reaction is in doubt, but two

$$M(CO)_4(CO_2H)^- + OH^- \underset{k_{-3}}{\overset{k_3}{\rightleftharpoons}} X \qquad (12)$$

logical possibilities are $M(CO)_4(CO_2)^{2-}$ or $M(CO)_3(CO_2H)_2^{2-}$.

(23) Walker, H.; Ford, P. C. *Inorg. Chem.* **1982**, *21*, 2509.
(24) Bender, M. L.; Clement, G. E.; Gunter, C. R.; Kezdy, F. J. *J. Am. Chem. Soc.* **1964**, *86*, 3697.

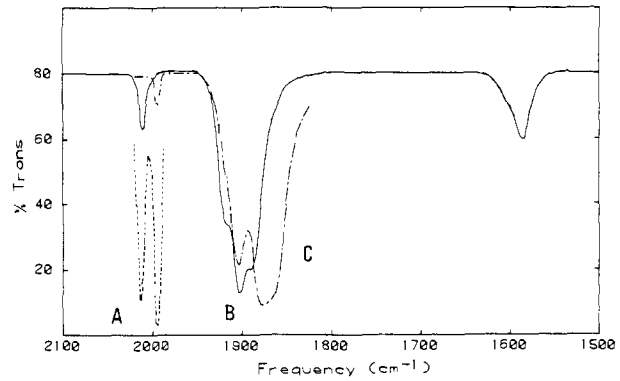

Figure 5. Infrared spectra (ν_{CO} region) of (A) $Fe(CO)_5$, (B), $Na[Fe(CO)_4(CO_2CH_3)]$, and (C) $Na[HFe(CO)_4]$ in THF solution.

It is not clear whether species X represents the terminus of a "dead-end" equilibrium or lies directly along the reaction coordinate for generation of $HM(CO)_4^-$. However, other evidence argues against the direct participation of X in the mechanism for formation of $HFe(CO)_4^-$ from $Fe(CO)_5$ in THF solutions (see below). Plots of k_{obsd} vs. [base] gave k_3 values of (57 ± 5) × 10^2 and (1.3 ± 0.2) × 10^2 M^{-1} s^{-1} for the iron and ruthenium systems, respectively, in aqueous THF.

The reactions of $(Bu_4N)OH$ with $M(CO)_5$ in aqueous THF were also investigated with the IR spectrophotometer equipped with a stopped-flow cell. The formation of $HRu(CO)_4^-$ from the reaction of $(Bu_4N)OH$ (3 to 30 × 10^{-3} M) with $Ru(CO)_5$ (1.5 × 10^{-3} M) in 90/10 THF/H_2O was monitored at the 1887-cm^{-1} absorbance band of the $HRu(CO)_4^-$ anion. The rate of $HRu(CO)_4^-$ formation was first order in [Ru] but independent of $[OH^-]$, with a measured rate constant (k_4) of 0.040 ± 0.006 s^{-1}.

The formation of $HFe(CO)_4^-$ under the same conditions was followed at three IR frequencies: 1990 cm^{-1} (corresponding to a CO band of $Fe(CO)_5$), 1874 cm^{-1} (a band of $HFe(CO)_4^-$), and 1905 cm^{-1} (wehre there is a maximum absorbance difference between $HFe(CO)_4^-$ and $Fe(CO)_4(CO_2CH_3)^-$ (Figure 5)). Given that the IR spectrum of $Fe(CO)_4(CO_2H)^-$ should be similar to that of the methoxide adduct, the absorbance at 1905 cm^{-1} should serve at an indication of the temporal concentration of $Fe(CO)_4(CO_2H)^-$. Upon mixing the $Fe(CO)_5$ and hydroxide solutions, it was found that the absorbance at 1990 cm^{-1} dropped to a low, constant value, indicating that the $Fe(CO)_5$ had reacted completely with OH^- during the mixing time of the instrument (~2 s). This observation is expected from the large k_2 values measured above. In contrast, a large initial absorbance at 1905 cm^{-1} was seen which subsequently decreased in intensity at a rate identical with the increase in absorbance at 1874 cm^{-1}. These observations imply that the species responsible for the 1905-cm^{-1} absorption, presumably $Fe(CO)_4(CO_2H)^-$, decays to give $HFe(CO)_4^-$. The rates for $HFe(CO)_4^-$ formation determined over the iron concentration ranges (1–3) × 10^{-3} M and base concentrations (6–100) × 10^{-3} M were first order in [Fe] but zero order in [base]. Rate constants for k_4 of 0.09 ± 0.02 and 0.07 ± 0.01 s^{-1} under CO and N_2 (1 atm), respectively, were obtained. Thus, formation of $HFe(CO)_4^-$ appears to be independent (within experimental uncertainty) of [CO] under these conditions.

A different reaction profile was seen in 90/10 CH_3OH/H_2O (Figure 6). Immediately after mixing the $Fe(CO)_5$ and hydroxide solutions in the stopped-flow IR apparatus, the strong absorbance at 1990 cm^{-1} attributed to $Fe(CO)_5$ was still present. This disappeared slowly with the same [base] dependent rate as the appearance of the 1890-cm^{-1} absorption of $HFe(CO)_4^-$. The initial absorbance at 1905 cm^{-1} was very small and increased at the same rate as that observed at 1890 cm^{-1}. The initial absorbance at 1905 cm^{-1} can be attributed to the presence of the intermediates $Fe(CO)_4(CO_2R)^-$ (R = H or CH_3) and/or to the product $HFe(CO)_4^-$. Thus, unlike the aqueous THF solutions described above, the concentrations of the adducts formed in aqueous methanol are very small. This observation is consistent with the small K_1 values measured in neat methanol for eq 9 (6.7 M^{-1}). The tem-

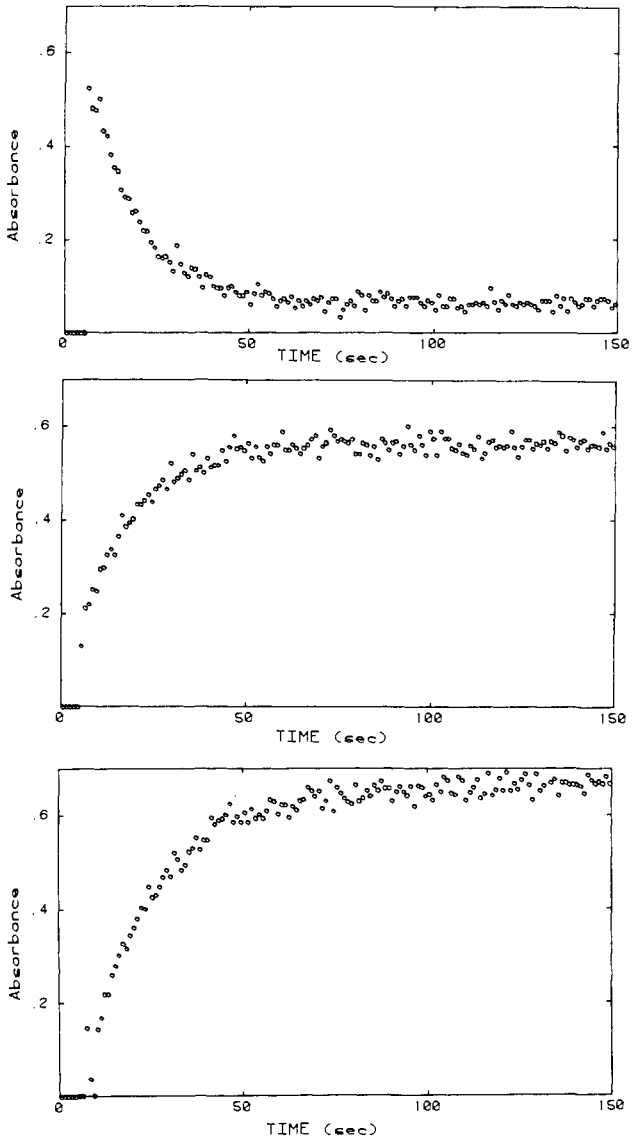

Figure 6. Time-dependent IR absorbance changes of a solution prepared from $Fe(CO)_5$ and $(Bu_4N)OH$ (0.01 M) in 90/10 CH_3OH/H_2O solution (~25 °C) monitored at 1990 (top), 1905 (middle), and 1890 cm^{-1} (bottom).

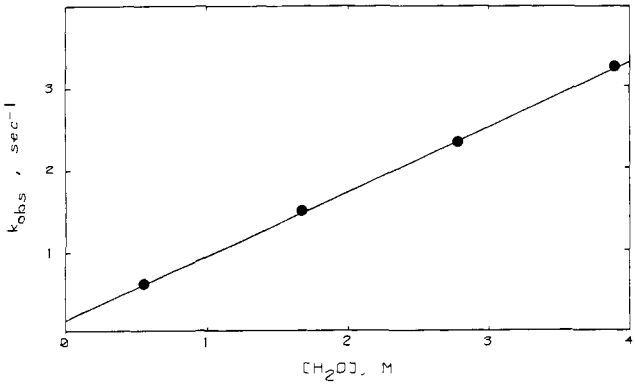

Figure 7. k_{obsd} vs. $[H_2O]$ for the formation of $HFe(CO)_4^-$ from the reaction of $Fe(CO)_5$ and base (0.105 M, introduced as $NaOCH_3$) in aqueous methanol (25.0 °C).

poral increase in the 1905-cm^{-1} absorbance (Figure 6) can be attributed to the formation of $HFe(CO)_4^-$.

The rate of $HFe(CO)_4^-$ formation in methanol with 0.1 M base was also found to be linear in $[H_2O]$ over the range 0.55 to 4.0 M (Figure 7). Although the equilibrium constants for adduct formation in this solvent system are small, it is reasonable to

Scheme II

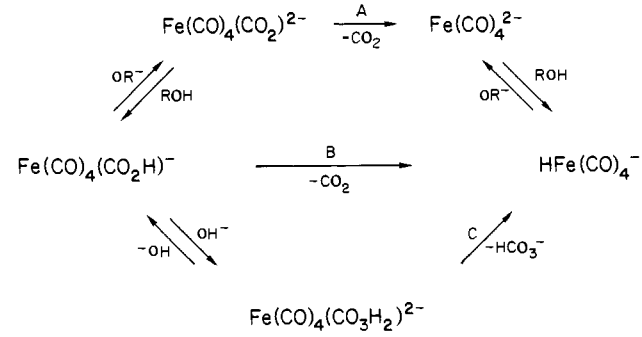

propose that $HFe(CO)_4^-$ formation occurs via the hydroxycarbonyl intermediate According to this mechanism, the rate would be

$$Fe(CO)_5 + OH^- \overset{K_2}{\rightleftharpoons} Fe(CO)_4(CO_2H)^- \quad (13)$$

$$Fe(CO)_4(CO_2H)^- \xrightarrow{k'} HFe(CO)_4^- + CO_2 \quad (14)$$

$$d[HFe(CO)_4^-]/dt = k'[Fe(CO)_4(CO_2H)^-] = k'K_2[OH^-][Fe(CO)_5] \quad (15)$$

In aqueous methanol, the total equivalents of base will be distributed between hydroxide and methoxide according to the reaction

$$CH_3O^- + H_2O \rightleftharpoons CH_3OH + OH^- \quad (16)$$

which has the equilibrium constant $K_b = 0.13$.[25] Given that $a(CH_3OH) \gg a(H_2O)$, $[OH^-]$ is proportional to the total base concentration $[OR^-]$. Equation 15 can then be rewritten as

$$d[HFe(CO)_4^-]/dt = k'K_bK_2[OR^-]R_a[Fe(CO)_5] \quad (17)$$

where R_a is the ratio of the solvent activities $a(H_2O)/a(CH_3OH)$. This rate law is consistent with the [base] dependence noted here and the first-order dependence of $[H_2O]$ (Figure 7) as well as the first-order dependence on [base] over the range 0.002 to 0.05 M reported previously for a similar, but not identical, solvent system (70/30 CH_3OH/H_2O).[10]

The question remains regarding the mechanism of eq 14. Several mechanisms have been proposed for the decarboxylation of hydroxycarbonyls. These are illustrated in Scheme II for the $Fe(CO)_4(CO_2H)^-$ anion. On the basis of nonlinearity of the base dependence of the rate of formation of $HFe(CO)_4^-$ at low base concentration (<0.002 M) in 70/30 CH_3OH/H_2O, earlier workers proposed[10] that the reaction proceeds via a deprotonation mechanism (Scheme IIA). Similar mechanisms have been proposed for other such decarboxylations of hydroxycarbonyls.[26] However, there are also reports on the relative stability of anionic metal CO_2 complexes compared to the hydroxycarbonyl analogue. These observations led to the conclusion that decarboxylation occurs via β-elimination of M–H from the $M-CO_2H$ functionality (Scheme IIB).[27] For example, Pettit and co-workers have shown[28] that while $(\eta^5\text{-}C_5H_5)Fe(CO)_2(CO_2H)$ will readily undergo decarboxylation when warmed in benzene solution the conjugate base $(\eta^5\text{-}C_5H_5)Fe(CO)_2(CO_2)^-$ in dry formamide solution does not decarboxylate, even when heated to 100 °C. A third mechanism suggested for a different system[29] involves addition of a second OH^- to the hydroxycarbonyl group to give a $C(OH)_2O$ function

(25) Koskikallio, J. *Suom. Kemistil. B* **1957**, *30*, 111, 115 as reported in ref 10.
(26) (a) Bercaw, J. E.; Goh, L. Y.; Halpern, J. *J. Am. Chem. Soc.* **1972**, *94*, 6534. (b) Sweet, J. R.; Graham, W. A. G. *Organometallics* **1982**, *1*, 982. (c) Darensbourg, D. J.; Froelich, J. A. *Inorg. Chem.* **1978**, *17*, 3300.
(27) (a) Catellani, M.; Halpern, J. *Inorg. Chem.* **1980**, *19*, 566. (b) Clark, H. C.; Jacobs, W. J. *Inorg. Chem.* **1970**, *9*, 1229.
(28) Grice, N.; Kao, S. C.; Pettit, R. *J. Am. Chem. Soc.* **1979**, *101*, 1627.
(29) Darensbourg, D. J.; Rokick, A. *Organometallics* **1982**, *1*, 1685.

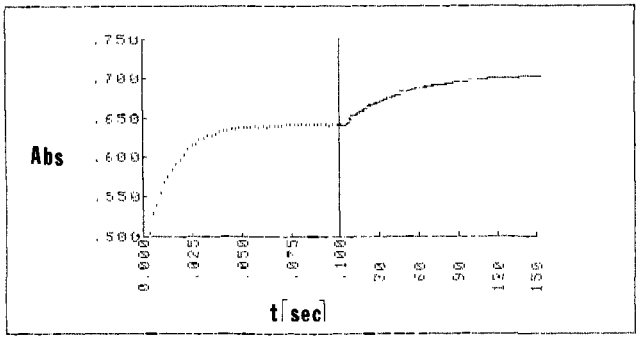

Figure 8. Absorbance (310 nm) vs. time plot for the reaction of $Fe(CO)_5$ with $(Bu_4N)OH$ (4.5 mM) in 50/48/2 $THF/CH_3OH/H_2O$ solution (25.0 °C). (Note that in the first part of the plot the time scale is 0.025 s/division while in the second part the scale is 30 s/division.)

which subsequently decomposes via loss of HCO_3^- (Scheme IIC).

The base independence of the decarboxylation rates in 90/10 THF/H_2O, where K_2 is very large and the decarboxylation can be observed directly, is consistent with operation under these conditions of the type of mechanism described in Scheme IIB but is inconsistent with the base dependence predicted for path A and B in Scheme II. In aqueous methanol where K_2 is small, direct observation of the decarboxylation from the hydroxycarbonyl adduct is precluded; therefore, it was decided to examine intermediate conditions similar to those commonly used in WGSR catalysis[7a] but where equilibrium constants for adduct formation are much larger than in methanol.

Reactions of $Fe(CO)_5$ with Base in $THF/CH_3OH/H_2O$ (50/48/2) Solutions. The reaction profile monitored by ν_{CO} changes in the stopped-flow IR spectrophotometer in this tertiary solvent system suggested the following scenario. First, a fast reaction occurs during the mixing time of the instrument, resulting in formation of a mixture of $Fe(CO)_5$, $Fe(CO)_4(CO_2CH_3)^-$, and $Fe(CO)_4(CO_2H)^-$, the ratio of $Fe(CO)_5$ to the two adducts depending upon the initial total base concentration. Second, there is a slower reaction involving the disappearance of these three species with the concurrent appearance of $HFe(CO)_4^-$. The reaction kinetics for the latter process were followed from the appearance of the 1874-cm^{-1} absorption. The observed rate showed dependence upon [total base] at lower concentrations (<0.02 M) but became independent of [total base] at higher concentrations (0.02 to 0.10 M), giving a limiting rate constant of ~ 0.13 s^{-1}.

These reactions were also followed quantitatively in the Durrum stopped-flow spectrophotometer at 310 nm. Upon mixing of the base (introduced as $(Bu_4N)OH$) and $Fe(CO)_5$ solutions, two sequential processes were observed. First, there was a fast reaction whose change in absorbance was dependent upon [base]. This was followed by a slower reaction which gave a final absorbance characteristic of the $HFe(CO)_4^-$ anion (Figure 8). These observations are consistent with theh rapid, competitive adduct formation to give an equilibrium mixture of $Fe(CO)_5$, $Fe(CO)_4(CO_2CH_3)^-$, and $Fe(CO)_4(CO_2H)^-$ followed by decay of this mixture to $HFe(CO)_4^-$. Rates of the initial spectral changes obeyed the rate law

$$\text{rate} = (k_f[\text{base}] + k_r)[Fe(CO)_5] \qquad (18)$$

over the base range 0.001 to 0.030 M (Table III). The values $k_f = (8.0 \pm 0.2) \times 10^3$ M^{-1} s^{-1}, $k_r = 37 \pm 2$ s^{-1}, and $K_{eq} = (2.0 \pm 0.2) \times 10^2$ M^{-1} compare well with the values for k_1, k_{-1}, and K_1 measured at 25 °C in 50/50 THF/CH_3OH (Table III). The subsequent slow formation of $HFe(CO)_4^-$ was also first order in [Fe] but gave the k_{obsd} vs. [base] profile shown in Figure 9.

In alkaline $THF/CH_3OH/H_2O$ solutions the base is present both as OH^- and as CH_3O^-. The latter should be favored because $a(CH_3OH) \gg a(H_2O)$ and K_b (eq 15), while unknown in this solvent system, can be expected to be small. As a consequence, addition of $Fe(CO)_5$ leads to the rapid formation of the equilibrium mixture of $Fe(CO)_5$, $Fe(CO)_4(CO_2CH_3)^-$, and $Fe(CO)_4(CO_2H)^-$ observable by IR spectroscopy which subsequently undergoes slow decay to form $HFe(CO)_4^-$. Under these conditions the rate law

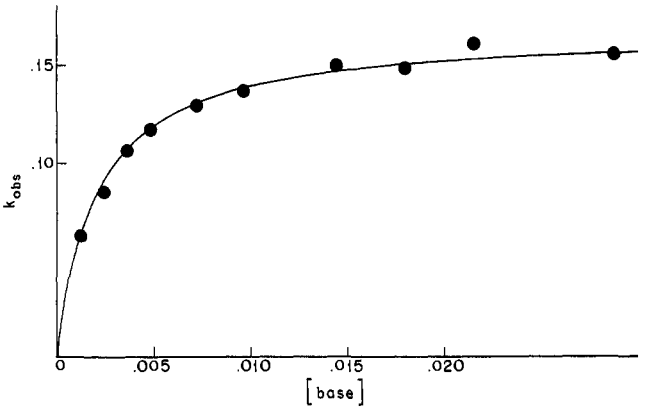

Figure 9. Plot of k_{obsd} vs. [base] (introduced as $NaOCH_3$) for the formation of $HFe(CO)_4^-$ from $Fe(CO)_5$ in 50/48/2 $THF/CH_3OH/H_2O$ solution (5.5 °C). Points indicated are experimental values and the curve represents the theoretical rate behavior based on the model (eq 26) with the values $K_1 = 500$ M^{-1} and $k_{obsd}(\text{lim}) = 0.167$ s^{-1}.

for decarboxylation via paths A and B in Scheme II can be derived as follows.

$$Fe(CO)_5 + OCH_3^- \underset{k_{-1}}{\overset{k_1}{\rightleftharpoons}} Fe(CO)_4(CO_2CH_3)^- \qquad (19)$$

$$Fe(CO)_5 + OH^- \underset{k_{-2}}{\overset{k_2}{\rightleftharpoons}} Fe(CO)_4(CO_2H)^- \qquad (20)$$

$$Fe(CO)_4(CO_2H)^- + OR^- \underset{k_{-3}}{\overset{k_3}{\rightleftharpoons}} Fe(CO)_4(CO_2)^{2-} + HOR \qquad (21)$$

$$Fe(CO)_4(CO_2H)^- \xrightarrow{k_e} HFe(CO)_4^- + CO_2 \qquad (22)$$

$$Fe(CO)_4(CO_2)^{2-} \xrightarrow{k_d} Fe(CO)_4^{2-} + CO_2 \qquad (23)$$

$$Fe(CO)_4^{2-} + H_2O \overset{\text{fast}}{\rightleftharpoons} HFe(CO)_4^- + OH^- \qquad (24)$$

According to Scheme IIA, eq 23 is the decarboxylation mode and the rate law would be

$$\frac{d[HFe(CO)_4^-]}{dt} = k_d[Fe(CO)_4(CO_2)^{2-}] = \frac{k_d K_b K_2 K_3 R_a [OR^-]^2[Fe]}{1 + (K_1 + K_2 K_b R_a)[OR^-]} \qquad (25)$$

where $[Fe] = [Fe(CO)_5] + [Fe(CO)_4(CO_2H)^{-1}] + [Fe(CO)_4(CO_2CH_3)^{-1}]$ and K_3 is small according to the IR experiments observed for this solvent system. This rate law predicts that at low $[OH^-]$ the reaction should be second order in base while first-order behavior should be evident at higher $[OH^-]$. A similar rate law is predicted for Scheme IIC. Since the kinetic behavior shown in Figure 9 clearly does not fit the prediction of eq 25, we conclude that neither path A or path C in Scheme II can be the dominant mechanism for decarboxylation under these conditions.

For Scheme IIB the rate law is

$$\frac{d[HFe(CO)_4^-]}{dt} = \frac{k_e K_2 K_b R_a [OR^-][Fe]}{1 + (K_1 + K_2 K_b R_a)[OR^-]} \qquad (26)$$

which can be simplified to $d[HFe(CO)_4^-]/dt = k_{obsd}[Fe]$ where

$$k_{obsd} = \frac{k_e K_2 K_b R_a [OR^-]}{1 + K_1[OR^-]} \qquad (27)$$

under the conditions studied here.[30] At low base concentrations this predicts k_{obsd} to have first-order dependence on $[OR^-]$, levelling

(30) Given the greater nucleophilicity of CH_3O^- toward the metal carbonyls (relative to OH^-), we may assume that $K_1 > K_2$ perhaps by as much as an order of magnitude. Furthermore, it seems unlikely that K_b (0.13 in aqueous methanol) will become substantially larger as the percentage of THF is raised, a more likely scenario being a decrease in K_b. Lastly $R_a < 1$ for all conditions investigated. Hence we conclude that in the mixed CH_3OH/H_2O or $THF/CH_3OH/H_2O$ solvents investigated $K_1 + K_2 K_b R_a \simeq K_1$.

off to base-independent values at higher [OR^-], exactly as seen in Figure 9. The double reciprocal plot $(k_{obsd})^{-1}$ vs. $[OR^-]^{-1}$ should be linear and have the intercept $K_1/(k_eK_2K_bR_a)$ and an intercept/slope ratio equal to K_1. The K_1 value obtained in this manner from the 5.5 °C data of Figure 9 is 500 M^{-1}, within experimental uncertainty of the k_f/k_r ratio measured for adduct formation. The limiting k_{obsd} at high [OR^-] equals (intercept)$^{-1}$, i.e., $k_eK_2K_bR_a/K_1$, in this case 0.167 s^{-1}. The theoretical curve of Figure 9 was calculated with these values. At 25 °C similar interpretation of experimental results gave K_1 = 200 M^{-1} and k_{obsd}(lim) = 0.15 s^{-1}. If one makes the assumption that K_b is about the same as in aqueous methanol (0.13 at 25 °C) and that R_a is equal to the molality ratio $(m(H_2O)/m(CH_3OH) = 0.1)$ then $k_eK_2/K_1 \cong 15$ in the 50/48/2 THF/CH_3OH/H_2O mixed solvent. Given further the indications that $K_2/K_1 < 1$ (see above), one can estimate that k_e is substantially greater than 1 s^{-1} in this solvent. By comparison in 90/10 THF/H_2O k_{obsd}(lim) (2.e., k_e under these conditions) for the formation of $HFe(CO)_4^-$ was measured to be 0.1 s^{-1} at 25 °C. Thus it appears that k_e is larger in the more protic solvent, an observation suggesting that water or methanol may somehow mediate the transfer of hydrogen from the hydroxycarbonyl oxygen to the metal. A similar observation has been made by Catellani and Halpern, who noted that the platinum hydroxycarbonyl complex *trans*-[$PtCl(CO_2H)(PEt_3)2$] underwent decarboxylation more rapidly in the presence of water than in dry, aprotic solvents.[27,31a]

Summary

The present article has extensively examined the kinetics of the reactions of the oxygen nucleophiles CH_3O^- and OH^- with the pentacarbonyl compounds $M(CO)_5$ to give the methoxy- and hydroxycarbonyl adducts. Relative to the reaction with free CO[32], those with coordinated CO are dramatically activated. The heavier metal pentacarbonyls are the more reactive, but replacement of one CO by PPh_3 led to a substantial deactivation of the remaining carbonyls toward adduct formation. Methoxide proved to be a more powerful nucleophile than hydroxide under comparable conditions and both nucleophiles were more reactive in less polar solvent mixtures despite probable ion pairing with the counterions. The methoxycarbonyl adducts were stable but hydroxycarbonyl analogs underwent decarboxylation to give the respective metal hydride anions $HM(CO)_4^-$. In aqueous THF or the THF/CH_3OH/H_2O mixed solvent, decarboxylation occurs by a base and P_{CO} independent pathway proposed to be a "unimolecular" β-elimination.[33] This step did appear to be sensitive to the nature of the solvent and occurred at a faster rate in solvent systems containing a larger concentration of protic species. Our data also suggest that the base dependence of the WGSR catalysis by iron carbonyl, as described by King et al[34], is the result of the small values of K_2 (eq 20) combined with the low pH under catalysis conditions.

Acknowledgment. This work was supported by a contract with the U.S. Department of Energy, Office of Basic Energy Sciences. The ruthenium used in these studies was provided on loan by Johnson-Matthey Inc.

(31) In this context, Squires and co-workers have recently found that in the gas phase a $Fe(CO)_5/OH^-$ adduct believed to be the hydroxycarbonyl complex is quite stable and does not readily undergo decarboxylation. (Lane, K. R.; Lee, R. E.; Sallans, L.; Squires, R. R., submitted for publication. Private communication from R. R. Squires.)

(32) Free CO reacts slowly with aqueous base at elevated temperatures (Iwata, M. *Chem. Abstr.* **1969**, *70*, 6989r).

(33) A referee has suggested that rate-limiting CO dissociation from $Fe(CO)_4(CO_2H)^-$ prior to decarboxylation would be consistent with the P_{CO} independence of this reaction. If this step were irreversible, the kinetics would indeed be indistinguishable from those expected for direct decarboxylation of $Fe(CO)_4(CO_2H)^-$.

(34) King, A. D.; King, R. B.; Yang, D. B. *J. Am. Chem. Soc.* **1980**, *102*, 1028.

High-Resolution Solid-State ^{27}Al and ^{29}Si Nuclear Magnetic Resonance Study of Pillared Clays

D. Plee,[†] F. Borg,[‡] L. Gatineau,[†] and J. J. Fripiat*[†]

Contribution from CRSOCI, CNRS, 45045 Orleans Cedex, France, and the Laboratoire de Recherches, CFR, Harfleur, France. *Received July 9, 1984*

Abstract: This paper aims to define the short-range order structure in smectites pillared with aluminum polyhydroxy polymers so as to produce acid catalysts or catalyst supports with specific surface areas on the order of 300 m^2/g and pore sizes on the order of 8 × 10 × 10 $Å^3$. For that purpose the ^{27}Al and ^{29}Si nuclear magnetic resonance spectra of pillared smectites without substitution in the tetrahedral layer (hectorite and laponite) or with substitutions in the tetrahedral layer (synthetic beidellite) have been recorded under the condition of magic angle spinning. In uncalcined samples, the main conclusion of this study is that the pillaring agent is the so-called Al_{13} polymer made from 12 Al octahedra surrounding 1 Al tetrahedron. When pillared smectites without tetrahedral substitution are calcined, there is no reaction between pillars and the smectite surface. On the contrary, in pillared beidellite a deep structural transformation occurs that can be interpreted as the growth of a tridimensional network grafted on the bidimensional network of the clay. The resulting high-area solid could be considered as a "bidimensional zeolite". Its acidic properties are indeed comparable with those of Y zeolites and much stronger than those of calcined pillared smectites without tetrahedral substitution.

The main purpose for pillaring a swelling clay is to keep a large fraction of the internal surface area available for adsorption and eventually for catalytic processes. Indeed smectites like dioctahedral montmorillonite or trioctahedral hectorite swell upon adsorbing polar reagents, but they lose their expanding properties after a heat treatment in a temperature range where adsorbent regeneration or catalytic reactions are carried out. The total surface areas (external plus internal) of swelling clays are close to the theoretical limit for a bidimensional sheet silicate, namely 800 m^2/g. The external surface area is usually lower than ~80 m^2/g. Since montmorillonite has been pillared with aluminum

[†] CRSOCI, CNRS.
[‡] Laboratoire de Recherches, CFR.

0002-7863/85/1507-2362$01.50/0